

The Case for 3D Visualization in DEM Assessment

Michael B. Gousie

Wheaton College, Norton, MA 02766, USA,
mgousie@wheatoncollege.edu,
WWW home page: <http://cs.wheatoncollege.edu/mgousie>

Abstract. The Digital Elevation Model, or DEM, is a common way to store elevation data. However, errors in various stages of DEM processing mean that the validity of a particular data point is uncertain. In many visualization systems, uncertainty in the data may be highlighted, but it is often difficult for the viewer to discern the exact nature of the problem. DEMView is a prototype DEM display system that incorporates several uncertainty visualizations, including curvature and local differences, while viewing the surface in two or three dimensions. The Profile Cutter and the magnifier are components of the system that allow the user to view a portion of the surface while keeping in the context of the overall area. In addition, the system displays visualizations for several quantitative uncertainty statistics. A detailed case study shows the efficacy of the system, especially the usefulness of viewing in three dimensions.

Keywords: DEM, visualization, uncertainty, focus plus context, 3D

1 Introduction

The digital elevation model (DEM), a file format in which elevation values are stored in a regular grid, is commonly used in computer geo-processing. Such data is utilized for many kinds of applications, including emergency route finding, flood plain determination, forest fire management, utility infrastructure, recreational development, and town planning. However, a DEM may be created for a particular geographic location via one of many methods, such as interpolating and/or approximating from contour or sparse data, converting LIDAR or shuttle radar topography mission (SRTM) data, or any number of other photogrammetry techniques. No matter how the DEM is computed, the accuracy of a particular point may be uncertain. Problems in a DEM can, in turn, lead to dramatic errors in applications that depend on the data. As an added consideration, because of the difficulty of determining the quality of a given DEM and the costs associated with procuring them, many users do not take into account possible errors [17], thus temporarily avoiding the issue until problems arise in the future.

Many GIS and other software can help users assess the quality of a DEM. However, many of these have a steep learning curve and produce visualizations

that are difficult and/or time consuming to evaluate. DEMView is a prototype system built solely for the purpose of viewing DEMs and assessing errors, and by its not having multiple layers of menus, is easier to navigate. It offers several quantitative and qualitative assessment tools, including visualizations in two or three dimensions, giving the user flexibility by offering various views that may help shed light on any potential problems in a DEM. A “profile cutter” and magnifier are two tools that allow the user to see small scale details in 2D within the context of a 3D visualization. A detailed case study is presented that highlights the major components of the system.

2 Related Work

The problem of assessing error and/or uncertainty in a DEM can be divided into two parts: (1) quantifying the error and (2) producing a visualization for assessed errors. Various approaches to ascertaining the extent of DEM error have been proposed [12], many of which are outlined below.

A standard uncertainty measure is the root mean square error (RMSE), which compares a DEM height point with a corresponding elevation from an accurate source [30]. Although it gives only a global measure of the validity of a DEM, recently Wise [35] found that RMSE of elevation is a good predictor of RMSE in gradient and aspect. Carrara et al. [6] use several analysis techniques, including determining if DEM heights fall between contour elevations. One way to test this is to create profile plots with the contour elevations highlighted [13], while another method is to use elevation histograms to show if there is a linear fit between contours [6, 29]. One can also compute the smoothness of a DEM by computing the total squared curvature [3] or, similarly, finding local curvature. Fisher [11] computed several statistics after comparing a DEM with established spot heights and computes a probable viewshed. Errors, based on grid bias, can be found by comparing drainage networks extracted by multiple rotations of the DEM [7]. Rigorous statistical models have been proposed as well [5]. Many of the above methods require the user to interpret the resulting error data. A visualization of the error gives the viewer immediate feedback to potential problems. Wood and Fisher [37] were early proponents of such visualizations; they compared several interpolated DEMs by displaying visualizations of aspect, Laplacian filtering that highlights sudden changes in elevation, RMSE, and shaded relief. While these give the viewer good insight not only to what the problems are but exactly where they lie, the visualizations were rendered in only two dimensions. Much work has been done in uncertainty visualization, such as using glyphs, translating/rotating surface patches to highlight potential error, altering lighting parameters, and so forth [27, 18]. Kao et al. show ways to visualize 2D probability distributions from geo-data sets [20, 23]. MacEachren et al. give a comprehensive overview of the state of visualizing uncertainty in geospatial domains [24].

There are many GIS that have good 3D visualization capability and at least some uncertainty visualization features, of which the following is a sampling.

Textures are shown to be useful for terrain visualization [9]. TerraFly [31] displays satellite imagery and other data in various resolutions. GeoZui3D [33] is a 3D marine GIS that supports multiple linked views; that is, the user can view the overall area and a smaller portion at much greater resolution. A GIS that integrates 2D and 3D views of the same data is described in [4]. A system that incorporates some error capabilities is LandSerf [36, 28], including shaded relief, curvature visualization, peak classification, and others. LandSerf is also very useful in generating contours and reading/writing many file formats. Another tool dedicated to displaying geographic areas and some errors using orthoimages is described in [34]. A thorough statistical comparison between a DEM computed from contours and new LIDAR shows that DEM error is indeed present and comes from several sources [26]. This work also shows the usefulness of visualizations in detecting and evaluating errors. VisTRE [14] is a system designed expressly for visualizing terrain errors. The work is guided by psychophysical studies to maximize the effectiveness of the visualizations while limiting perceptual biases.

3 DEMView Assessment and Visualization Tools

DEMView is a prototype system for DEM uncertainty visualization in two and three dimensions, written in C++ with the OpenGL Application Programming Interface (API) for the graphics rendering, the OpenGL Utility Toolkit (GLUT) for the window system and stenciling (see below), and FLTK (Fast Light Toolkit) [10] for the graphical user interface (GUI). Figure 1 shows the system displaying a 1000×1200 10-meter DEM taken from the 7.5' USGS National Elevation Dataset (NED) covering Franconia, NH. Elevations are in feet. The program reads data files in standard ArcInfo ASCII grid format. The default visualization shows the surface in green shaded-relief, with gray in areas above user-defined tree line elevation as well as in steep-slope terrain. Turning the green background off yields an all-gray shaded relief map.

A feature of the system is that the GUI is designed specifically for visualizing uncertainty in DEMs, somewhat following the model used by LandSerf except that the results of all operations can be viewed on the surface in three dimensions. All available features are displayed on the right panel at all times (unless hidden by user); they are all available through menus as well. Options that are grayed-out require a second comparison DEM (see below) for activation. Rotation of the 3D surface is accomplished through the left mouse button and translation through the right button. Zooming can be done using the panel buttons or the scroll button on a mouse. Other panel buttons provide common rotations/translations with one-click functionality. Contour, sparse, or full DEM data can be used to compare with the subject DEM, with various ways to display both data sets simultaneously as described below. In all cases, no special scripts or multiple levels of menus are required.

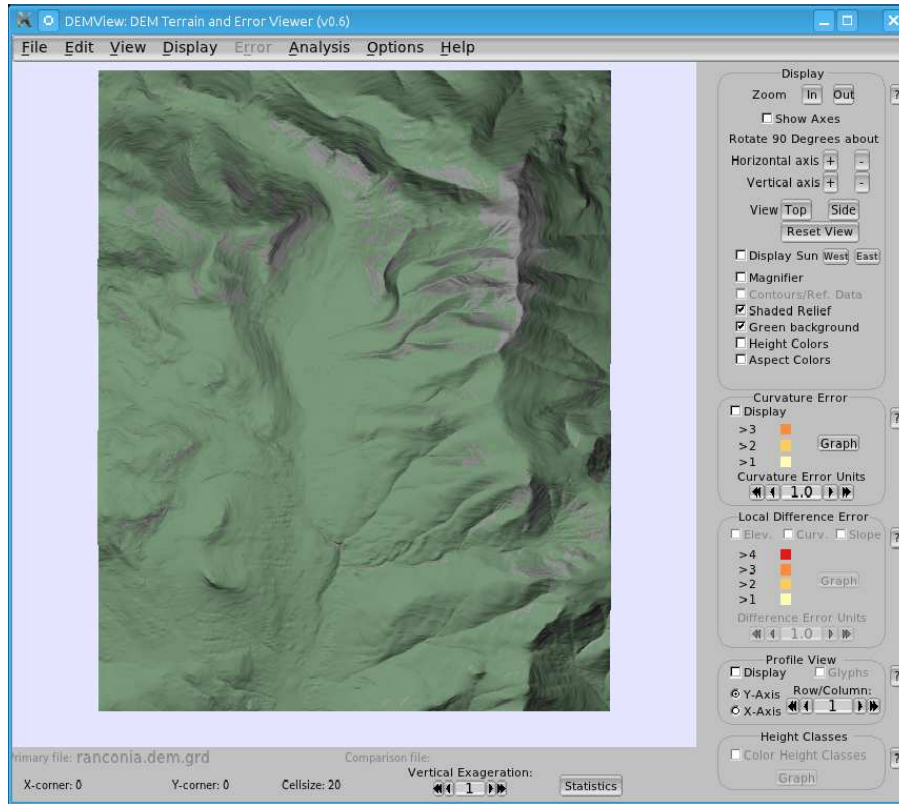


Fig. 1. Default view of Franconia DEM on DEMView. Note GUI panel on right showing all options.

3.1 Curvature and Local Difference Error Visualization

The overall smoothness of a DEM can be computed by finding the total squared curvature, C_{sq} [3]:

$$C_{sq} = \sum \sum (u_{i+1,j} + u_{i-1,j} + u_{i,j+1} + u_{i,j-1} - 4u_{i,j})^2 \quad (1)$$

The total squared curvature may be biased if there are large problem areas in a DEM. To mitigate this, an indication of local smoothness can be found by averaging the local, or absolute, curvature which is found at a point i, j :

$$C_{abs} = |(u_{i+1,j} + u_{i-1,j} + u_{i,j+1} + u_{i,j-1} - 4u_{i,j})| \quad (2)$$

The value of C_{abs} is the curvature at a specific point. Severe curvature may indicate an error in the DEM; patterns in curvature may indicate systematic errors due to interpolation. Such curvature error can be displayed in DEMView,

where the threshold is chosen by the viewer. The curvature is displayed via different hues, where the green surface indicates no error (little curvature) and progressing through yellow to orange for the highest error (extreme curvature). The colors were chosen in accordance with other visualization systems [14] and color perception studies [8]. The user may choose to have these errors categorized into clear levels or displayed via a change in hue proportional to the error. The GUI labels change dynamically to indicate the current level of error relative to the displayed colors.

To visualize discrepancies between source data and DEM, each source height point is compared to the corresponding elevation in the DEM to find the local difference error d at point i, j :

$$d_{i,j} = |u_{i,j} - v_{i,j}| \quad (3)$$

where v is the elevation in the comparison DEM. Following [6], d should not be greater than 5% of the contour interval. Thus, similar to the mechanism described for curvature error, colors are assigned to elevations that have d greater than 5%, 10%, and so forth. If the comparison data is sparse data or another DEM, the user can indicate an appropriate level of error.

3.2 Height Class Frequency Visualization

If the source data is contours, then the DEM values within an area bounded by a contour pair should vary almost linearly, indicating an absence of artifacts such as terracing. DEM elevations are grouped into integer intervals between two contours and then reclassified into relative elevations [6]. For example, if 1200-1220 represents a contour pair, then the relative elevations, or height classes, would be 0, 1, 2, ..., 19 corresponding to the elevations of 1200, 1201, 1202, ..., 1219. The height classes are computed and the surface is displayed in green with the absolute frequency of the relative heights shown in graduated color from green to orange. The brighter the orange, the higher the absolute frequency of that height class, indicating that the slope is not linear between successive contours. The actual absolute frequencies are displayed as well for graphing purposes. It must be noted that the absolute frequency is a global measure that is applied to individual points, and thus the visualization is only a guide as to where errors may be. In other words, all points with the same color indicate they are all in the same height class. Ideally, there should be no orange in the surface at all.

3.3 Quantitative Statistics

The user can also opt to have DEMView display various statistics. These include total squared curvature, maximum curvature, and the count for each of the curvature error levels (which can also be shown as a graph), along with other standard summary statistics. If the DEM is being compared to another DEM or sparse data, comparison statistics are computed as well. These include the counts for difference error levels and the RMSE. Additional statistics will be included in future versions of the system.

4 Focus Plus Context

DEMView supports two tools that allow the user to focus on a small portion of a DEM while keeping the surface in context. The Profile Cutter and the magnifier can be used in conjunction with any other visualizations described above.

4.1 The Profile Cutter

While many systems offer visualizations that enable the viewer to see errors in general, it is often difficult to zoom in on a small area to ascertain minute differences between a DEM and comparison data. The Profile Cutter is a semi-transparent planar rectangle that is orthogonal to the surface. The cutter enables the viewer to make a vertical “slice” through the DEM to better see the profile at any x or y position. The position can be changed dynamically through buttons on the GUI, including moving the profile incrementally. Alpha blending makes the cutter semi-transparent, thus showing the profile within the context of the remaining DEM in the background. We also implemented what might be called “full context;” that is, showing the DEM portion in front of the Profile Cutter as a semi-transparent surface, but this made the visualization too cluttered.

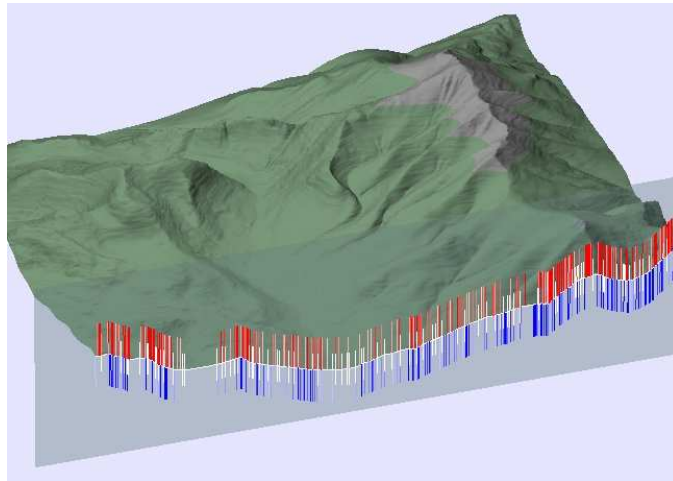


Fig. 2. The Profile Cutter slicing through the Franconia DEM.

The power of the Profile Cutter is more apparent when the primary DEM is being compared to another data set, be it sparse or another full DEM. The profile that is shown in white is always that of the primary DEM. In the comparison data set, if there exists a valid elevation at an x, y position, then a glyph can be displayed in the profile. The glyph is a vertical line segment of constant length that has the following properties:

- If the primary and secondary elevations match within a user-specified threshold, then the glyph is rendered in white vertically centered at the profile.
- If the elevation in the primary DEM is below the elevation in the secondary, then the glyph is rendered in a red hue proportional to the difference of the two elevations, where almost white indicates a slight difference and bright red indicates a large difference. In addition, the bottom endpoint of the line segment is at the elevation contained in the secondary data set.
- If the elevation in the primary DEM is above the elevation in the secondary, then the glyph is rendered in shades of blue, with dark blue indicating a large difference. The endpoint at the top of the line segment is at the elevation contained in the secondary data set.

Figure 2 shows the Profile Cutter slicing through the Franconia DEM compared to contour data. The glyphs show how well the contour elevations match the DEM. More examples of the Profile Cutter are shown in the case study.

4.2 The Magnifier

The newest tool in the system, and still in its early stages, is the magnifier. This tool enables the viewer to zoom in on just one portion of the DEM and any enabled visualizations being viewed in three dimensions, thereby keeping this zoomed area within the context of the overall terrain. This may be useful in getting a closer look at a possible problem area without losing one's place in the DEM. This idea comes from Magic Lenses [2], which could not only magnify but could also be used as an effective interface tool. A 3D version was implemented soon afterward [32]. Looser et al. extended the lenses for augmented reality interfaces [22]. Detail lenses, a similar idea for zooming in on areas for route visualization is described in [21], but its use is limited to 2D. Studies have also shown that semantic lensing and/or focus plus context are beneficial for tasks similar to what is being presented here [1, 19]. The magnifier is activated by pressing the appropriate button; clicking on the middle button or scroll wheel positions and/or drags the magnifier. The area within the magnifier is enlarged by a factor of two. The amount of zoom will be user-defined in future versions. The underlying visualization continues to be in 3D, and all transformation functions are available, allowing the user to dynamically change the viewing position with the magnifier on.

The implementation of the magnifier uses a stencil buffer. The user positions the cursor on the DEM; from this position a rectangular window is defined. The entire surface is zoomed but is then clipped to the window. Thus, only the zoomed portion is rendered (along with the original DEM behind), offering dynamic performance. A circular magnifier, in keeping with many people's notion of a hand-held magnifier, has been studied, but its implementation may be too inefficient for reasonable performance.

The use of the magnifier is demonstrated in the Case Study, below.

5 Case Study

Consider Figure 3, an 800×800 DEM with one meter resolution constructed from a USGS DLG of Mt. Washington, NH, with 20 meter contour intervals. This mountain has the distinction of being the highest peak in the Northeast United States as well as having a dangerous reputation because of severe weather and avalanche danger. In fact, 13 people have died on the mountain since 1956 due to avalanches [25]. Several deaths have occurred in the Tuckerman Ravine area, a popular spring skiing venue that often exhibits dangerous snow conditions. One may wish to investigate the terrain in that area to determine the causes of those avalanches.

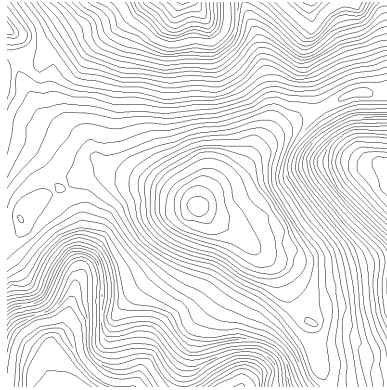


Fig. 3. Contours of Mt. Washington; Tuckerman Ravine is shown in the SW corner.

Now further suppose that the aforementioned contours are the sole data available. In order to investigate the area more fully, two DEMs were produced by interpolating the contours using two methods: TOPOGRID [16, 15], a well-known and reliable method available in Arc/Info, and an algorithm whereby intermediate contours (INTERCON) are first generated before interpolating [13]. Figure 4 shows the TOPOGRID surface while Figure 5 shows the INTERCON DEM. In both cases, the DEMView displays gray above the 4500 foot treeline and green below; note that this feature can be toggled. Looking at the two figures, there are clearly differences between the two DEMs. Which one should be used for further study? The next sections describe the functionality of DEMView and show the effectiveness of the three-dimensional viewing.

5.1 Preliminary Statistics

In order to do a preliminary assessment, the TOPOGRID and INTERCON DEMs were loaded into DEMView along with the original contours. Table 1 shows the relevant statistics. The RMSE shows the fit of each DEM with the

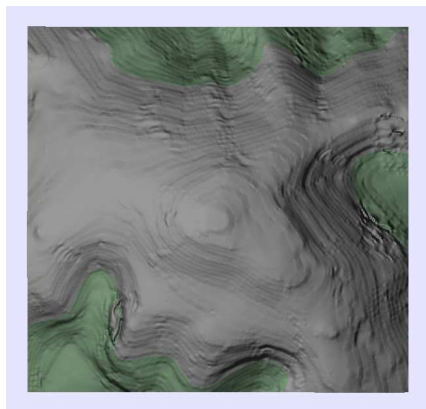


Fig. 4. TOPOGRID DEM of Mt. Washington.

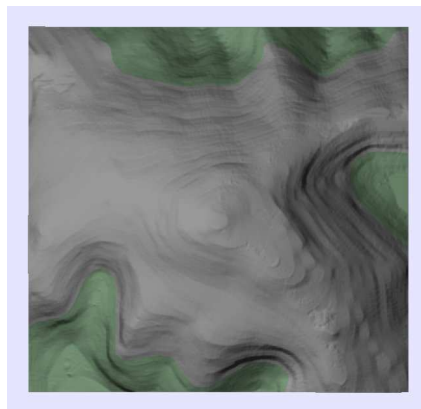


Fig. 5. INTERCON DEM of Mt. Washington.

Table 1. Statistical comparison of TOPOGRID and INTERCON DEMs.

| Statistic | TOPOGRID | INTERCON |
|-----------------------------------|-----------|----------|
| RMSE | 3.39 | 1.19 |
| Total C_{sq} | 134142.30 | 18582.44 |
| Max C_{abs} | 30.24 | 2.73 |
| Average C_{abs} | 0.21 | 0.03 |
| Curvature class counts | | |
| > 3.0 | 1732 | 0 |
| > 2.0 | 2368 | 117 |
| > 1.0 | 15742 | 2104 |
| Elevation difference class counts | | |
| > 4.0 | 3669 | 550 |
| > 3.0 | 1127 | 577 |
| > 2.0 | 1721 | 2252 |
| > 1.0 | 3578 | 11007 |

original contours; INTERCON is clearly better, but not an exact interpolation of the data. The total squared curvature is also much less than TOPOGRID's, corroborating the visual sense of smoothness. The curvature class counts reflect the number of points that have a local curvature of over three, over two, and over one. These counts reflect the overall curvature, or roughness, that can be seen in Figures 4 and 5. The elevation difference class counts show the number of points that deviate by more than four meters, more than three meters, etc. Interestingly, the TOPOGRID surface has fewer points in total that deviate from the original contour data, but for those points that do, there are a significant number whose local differences are much worse than INTERCON's. But *where* are the differences? If we wish to study an avalanche area, it is crucial to know

where the DEM problems may lie. Figures 6 and 7 show DEMView’s curvature visualization turned on. The colors change from yellow (low curvature) to bright orange (high curvature). Clearly, there is much more local curvature in the TOPOGRID DEM. Similarly, Figures 8 and 9 show the TOPOGRID and INTERCON DEMs with the local difference visualization turned on. The results are much the same; that is, the TOPOGRID surface shows more points with a high elevation difference compared to the original contour data. While these tools show that there is indeed some anomaly in the TOPOGRID DEM especially, it is not visually clear what the problem may be.

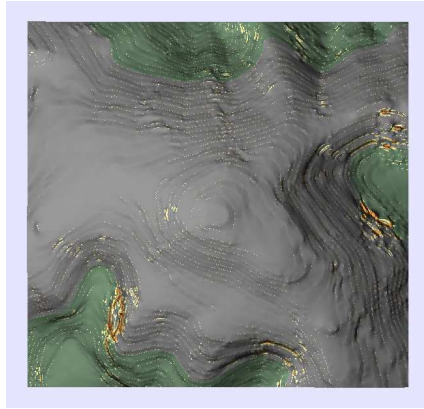


Fig. 6. TOPOGRID showing curvature. Colors range from yellow (low curvature) to orange (high curvature). Note problematic section in SW corner.

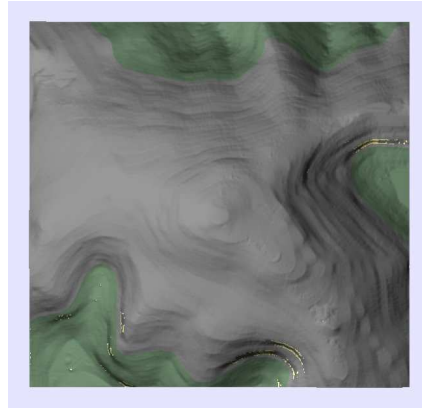


Fig. 7. INTERCON showing far less curvature than TOPOGRID.

5.2 3D Visualization Tools

Although much statistical and visualization analysis can be done with DEMs shown only in two dimensions, it may be beneficial to give the user the option of viewing in three dimensions. This extra functionality may shed more light on a particular problem area of a DEM. For example, Figure 10 shows a zoomed and rotated view of the Tuckerman Ravine area of Figure 8. This now clearly demonstrates the strange “bulge” that was a result of the TOPOGRID interpolation; furthermore, the interpolation artifacts along the contours themselves are more easily visible.

Another functional aspect of DEMView is the ability to layer two DEMs on top of one another and then compute and display the local elevation differences and local curvature differences. Figure 11 shows elevation differences between the TOPOGRID and INTERCON DEMs. The obvious red section shows major

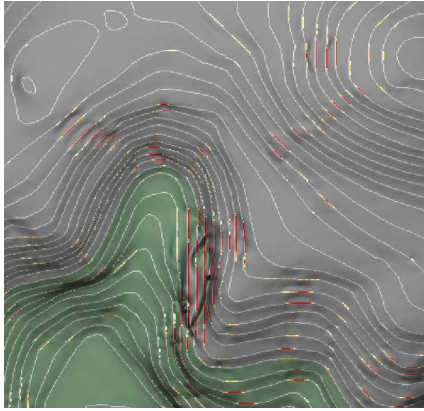


Fig. 8. DEMView displaying elevation differences between zoomed SW corner of the TOPOGRID DEM and underlying contours (shown in gray). Colors range from yellow (small difference) to red (large difference).

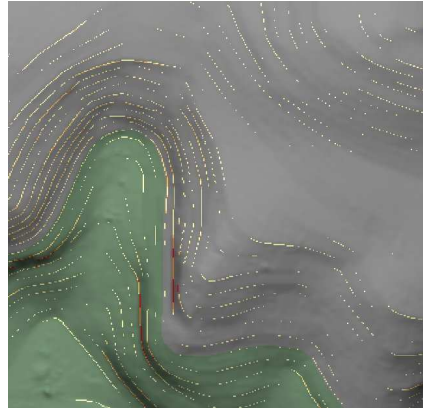


Fig. 9. INTERCON showing less drastic elevation differences but in higher quantity.

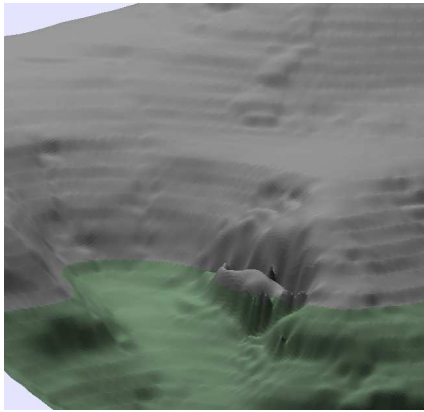


Fig. 10. Rotated and zoomed view of Tuckerman Ravine.

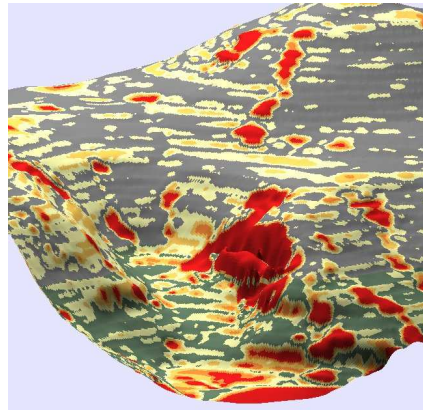


Fig. 11. Elevations differences between TOPOGRID and INTERCON.

differences between the elevations of the two DEMs in that area (refer back to Figure 9).

Finally, another use of three-dimensional visualization is shown in Figures 12 and 13. The former shows the Profile Cutter slicing through the problem area. Note that a) the surface behind the cutter provides context of where the profile is being cut; this is much better than many systems that allow for profiles but not in context (LandSerf for example), and b) both the TOPOGRID (in white) and the INTERCON profiles (in blue and red) are shown simultaneously. Thus the viewer can ascertain that the INTERCON surface has a much more natural curve in that area than the TOPOGRID DEM. The latter figure shows the same profile but with the glyphs turned on. This example shows all of the possibilities: the white glyphs represent agreement between the two DEMs, the shaded red glyphs (redder = larger difference) indicate that the primary file (TOPOGRID in this case) has lower elevations than the comparison DEM (INTERCON), and shaded blue glyphs indicate higher elevations in the primary DEM.

In all of these views, it would seem that the INTERCON DEM is better suited for further study of the Tuckerman Ravine area, as the surface exhibits fewer anomalies.

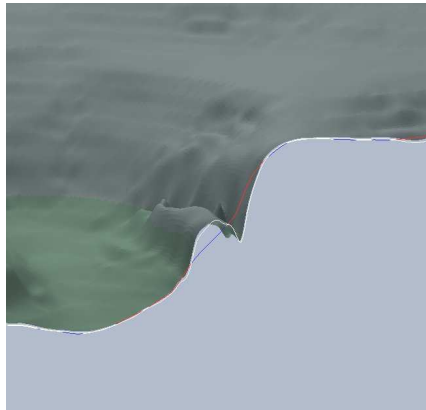


Fig. 12. Profile Cutter showing profiles of TOPOGRID (white) and INTERCON (DEMs).

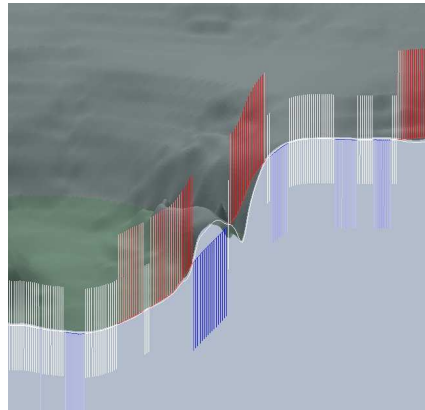


Fig. 13. Same comparison as in Figure 12, but with glyphs turned on. The brightness of the colors indicate the magnitude of the elevation difference.

6 Conclusion and Future Work

Here we have presented DEMView, a DEM and error visualization system. The curvature and local difference visualizations aid the user in finding areas of uncertainty in a DEM. The Profile Cutter can help the user more clearly see the

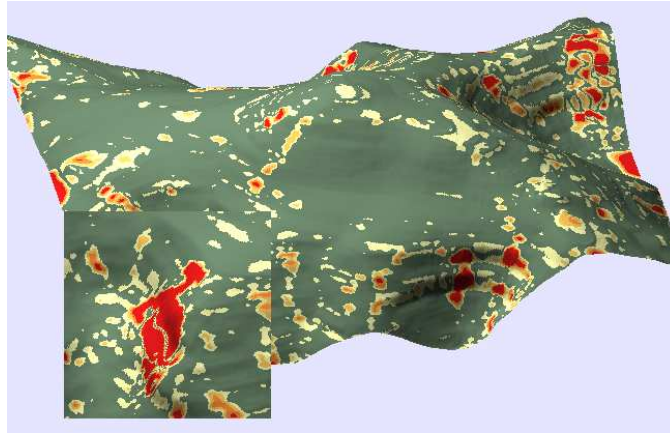


Fig. 14. Comparison of two DEMs of Mt. Washington with magnifier turned on; red indicates areas with a poor match between the two.

anomalous regions, as well as compare one DEM to another in a very specific area, all while keeping in context of the entire surface. The magnifier further aids the visualization. In using the tools, especially in conjunction with 3D viewing that afford additional information not seen in 2D, users can better decide how well a DEM suits their needs. Furthermore, all of DEMView’s functionality are easily accessible through the right panel, obviating the need to search through menus, etc.

In the future, additional visualizations of spatial statistics will be investigated. The magnifier is of special interest; current and new uncertainty visualizations could be rendered through the magnifier window, similar to Magic Lenses [2], allowing the user to remain in context at all times while affording dynamic “browsing” with the mouse over the surface. Another idea is to have the system find a cluster of local error and automatically focus on such an area with the magnifier tool. Finally, robust user studies would be useful to quantitatively determine the system’s ease of use.

References

1. Baudisch, P., Good, N., Bellotti, V., Schraedley, P.: Keeping things in context: a comparative evaluation of focus plus context screens, overviews, and zooming. In: CHI '02: Proceedings of the SIGCHI conference on human factors computing systems: Changing our world, changing ourselves. pp. 259–266. ACM (2002)
2. Bier, E.A., Stone, M.C., Pier, K., Buxton, W., DeRose, T.D.: Toolglass and magic lenses: the see-through interface. In: SIGGRAPH '93: Proceedings of the 20th annual conference on computer graphics and interactive techniques. pp. 73–80. ACM (1993)
3. Briggs, I.: Machine contouring using minimum curvature. *Geophysics* 39(1), 39–48 (February 1974)

4. Brooks, S., Whalley, J.L.: A 2d/3d hybrid geographical information system. In: Proceedings of ACM GRAPHITE. pp. 323–330. Dunedin, New Zealand (2005)
5. Carlisle, B.H.: Modelling the spatial distribution of DEM error. *Transactions in GIS* 9(4), 521–540 (2005)
6. Carrara, A., Bitelli, G., Carla', R.: Comparison of techniques for generating digital terrain models from contour lines. *International Journal of Geographical Information Science* 11(5), 451–473 (1997)
7. Charleux-Demargne, J., Puech, C.: Quality assessment for drainage networks and watershed boundaries extraction from a digital elevation model (dem). In: 8th ACM Symposium on GIS. pp. 89–94. Washington, D.C. (2000)
8. CIE: CIE Publication No. 15, Supplement Number 2 (E-1.3.1, 1971): Official Recommendations on Uniform Color Spaces, Color-Difference Equations, and Metric Color Terms. Commission Internationale de L'Éclairage (1978)
9. Döllner, J., Baumann, K., Hinrichs, K.: Texturing techniques for terrain visualization. In: Proceedings of the 11th IEEE Visualization Conference (VIS 2000). pp. 227–234 (2000)
10. Easy Software Products: FLTK: Fast light toolkit, <http://www.ftk.org/index.php>, <http://www.ftk.org/index.php>; last accessed 13 March 2007
11. Fisher, P.: Improved modeling of elevation error with geostatistics. *GeoInformatica* 2(3), 215–233 (1998)
12. Fisher, P.F., Tate, N.J.: Causes and consequences of error in digital elevation models. *Progress in Physical Geography* 30(4), 467–489 (2006)
13. Gousie, M.B., Franklin, W.R.: Augmenting grid-based contours to improve thin plate DEM generation. *Photogrammetric Engineering & Remote Sensing* 71(1), 69–79 (2005)
14. Healey, C.G., Snoeyink, J.: Vistre: A visualization tool to evaluate errors in terrain representation. In: Proceedings, 3rd International Symposium on 3D Data Processing, Visualization and Transmission (3DPVT 2006). Chapel Hill, North Carolina (2006)
15. Hutchinson, M.F., Gallant, J.C.: Representation of terrain. In: Longley, Goodchild, Maguire, Rhind (eds.) *Geographical Information Systems: Principles and Technical Issues*, vol. 1, pp. 105–124. Wiley, 2 edn. (1999)
16. Hutchinson, M.F.: Calculation of hydrologically sound digital elevation models. In: Proceedings of the Third International Symposium on Spatial Data Handling. pp. 117–133. International Geographical Union, Columbus, Ohio (1988)
17. Januchowski, S., Pressey, R., VanDerWal, J., Edwards, A.: Characterizing errors in digital elevation models and estimating the financial costs of accuracy. *International Journal of Geographical Information Science* 24(9), 1327–1347 (2010)
18. Johnson, C.R., Sanderson, A.R.: A next step: Visualizing errors and uncertainty. *IEEE Computer Graphics & Applications* 23(5), 6–10 (2003)
19. Kalghatgi, N., Burgman, A., Darling, E., Newbern, C., Recktenwald, K., Chin, S., Kong, H.: Geospatial intelligence analysis via semantic lensing. In: CHI EA '06: CHI '06 extended abstracts on human factors in computing systems. pp. 935–940. ACM (2006)
20. Kao, D., Dungan, J.L., Pang, A.: Visualizing 2d probability distributions from eos satellite image-derived data sets: A case study. In: VIS '01: Proceedings of the Conference on Visualization '01. pp. 457–461. IEEE (2001)
21. Karnick, P., Cline, D., Jeschke, S., Razdan, A.: Route visualization using detail lenses. *IEEE Transactions on Visualization and Computer Graphics* 16(2), 235–247 (March/April 2010)

22. Looser, J., Billinghamurst, M., Cockburn, A.: Through the looking glass: the use of lenses as an interface tool for augmented reality interfaces. In: GRAPHITE '04: Proceedings of the 2nd international conference on computer graphics and interactive techniques in Australasia and South East Asia. pp. 204–211. ACM (2004)
23. Luo, A., Kao, D., Pang, A.: Visualizing spatial distribution data sets. In: VIS-SYM '03: Proceedings of the Symposium on Data Visualization 2003. pp. 29–38. Eurographics Association (2003)
24. MacEachren, A.M., Robinson, A., Hopper, S., Gardner, S., Murray, R., Gahegan, M., Hetzler, E.: Visualizing geospatial information uncertainty: What we know and what we need to know. *Cartography and Geographic Information Science* 32(3), 139–160 (2005)
25. Mount Washington Observatory: Surviving mount washington (6/2012), <http://www.mountwashington.org/about/visitor/surviving.php>
26. Oksanen, J., Sarjakoski, T.: Uncovering the statistical and spatial characteristics of fine topographic DEM error. *International Journal of Geographical Information Science* 20(4), 345–369 (2006)
27. Pang, A.T., Wittenbrink, C.M., Lodha, S.K.: Approaches to uncertainty visualization. *The Visual Computer* 13(8), 370–390 (1996)
28. Raper, J., Dykes, J., Wood, J., Mountain, D., Krause, A., Rhind, D.: A framework for evaluating geographical information. *Journal of Information Science* 28(1), 51–62 (2002)
29. Reichenbach, P., Pike, R.J., Acevedo, W., Mark, R.K.: A new landform map of Italy in computer-shaded relief. *Bollettino Geodesia e Scienze Affini* 52, 22–44 (1993)
30. Rinehart, R.E., Coleman, E.J.: Digital elevation models produced from digital line graphs. In: Proceedings of the ACSM-ASPRS Annual Convention. vol. 2, pp. 291–299. American Congress on Surveying and Mapping, American Society for Photogrammetry and Remote Sensing (1988)
31. Rishe, N., Sun, Y., Chekmasov, M., Andriy, S., Graham, S.: System architecture for 3d terrain online GIS. In: Proceedings of the IEEE Sixth International Symposium on Multimedia Software Engineering (MSE2004). pp. 273–276 (2004), terrafly.com
32. Viega, J., Conway, M.J., Williams, G., Pausch, R.: 3d magic lenses. In: UIST '96: Proceedings of the 9th annual ACM symposium on user interface software and technology. pp. 51–58. ACM (1996)
33. Ware, C., Plumlee, M., Arsenault, R., Mayer, L.A., Smith, S.: Geozui3d: Data fusion for interpreting oceanographic data. In: Proceedings of the MTS/IEEE Conference and Exhibition (OCEANS 2001). vol. 3, pp. 1960–1964 (2001)
34. Wiggenghagen, M.: Development of real-time visualization tools for the quality control of digital terrain models and orthoimages. In: International Archives of Photogrammetry and Remote Sensing (IAPRS). vol. 33, pp. 987–993. Amsterdam (2000)
35. Wise, S.: Cross-validation as a means of investigating DEM interpolation error. *Computers & Geosciences* 37, 978–991 (2011)
36. Wood, J.D.: The Geomorphological Characterisation of Digital Elevation Models. Ph.D. thesis, University of Leicester, UK (1996)
37. Wood, J.D., Fisher, P.F.: Assessing interpolation accuracy in elevation models. *IEEE Computer Graphics and Applications* 13(2), 48–56 (March 1993)